Tokamak Magneto-Hydrodynamics (TMHD) for understanding and simulations of plasma disruptions*

Leonid E. Zakharov[1]
[1] ***Princeton University, PPPL, MS-27, PO Box 451, Princeton NJ 08543***

in collaboration with Xujing Li and Sergei Galkin

PPPL Theory Seminar
November 13, 2014, Princeton NJ

*This work is supported by US DoE contract No. DE-AC02-09-CH11466

Contents

Abstract

The simplest set of Tokamak Magneto-Hydrodynamics (TMHD) equations, sufficient for disruption modelling and expandable to more refined physics, is presented.

First, the TMHD introduces the 3-D Reference Magnetic Coordinates (RMC), which are aligned with the magnetic field in the best possible way. Being consistent with the high anisotropy of the tokamak plasma, RMC allow simulations at realistic, very high plasma electric conductivity and with high resolution of the plasma edge and resonant layers.

Second, the TMHD splits the equation of motion into an equilibrium equation and the plasma advancing equation. This resolves the 4 decade old problem of Courant limitations of the time step in existing, plasma inertia driven numerical codes.

Third, all TMHD equations have an energy principles, which lead to equations with positively defined symmetric matrices, thus, providing stability of numerical schemes.

The TMHD model was used for creation of theory of the Wall Touching Kink and Vertical Modes (WTKM and WTVM), prediction of Hiro and Evans currents, for initiation of Hiro current measurements on EAST, for designing an innovative diagnostics for tile current measurements on NSTX-U.

While Hiro currents have explained the toroidal asymmetry in the plasma current measurements in JET disruptions and sideways forces, the recently developed Vertical Disruption Code (VDE) have confirmed also the generation of Evans currents, which explain the tile current measurements in tokamaks.

Numerical simulations of WTVM have challenged the 24 years long misinterpretation of experimental measurements of the tile currents in tokamaks as "halo" currents, which have no even current carriers.

1 MHD models

Equation of motion

$$\rho \frac{d\mathrm{V}}{dt} = -\nabla p + (\mathrm{j} \times \mathrm{B}). \tag{1.1}$$

Equation of state

$$\frac{dp}{dt} = -\gamma p (\nabla \cdot \mathrm{V}), \quad \frac{d\rho}{dt} = -\rho (\nabla \cdot \mathrm{V}). \tag{1.2}$$

Ampere's law

$$\mathrm{B} = (\nabla \times \mathrm{A}), \quad \mu_0 \mathrm{j} = (\nabla \times \mathrm{B}). \tag{1.3}$$

Faraday's law

$$-\frac{\partial \mathrm{A}}{\partial t} + (\vec{V} \times \vec{B}) - \nabla \phi^E = \eta \mathrm{j}. \tag{1.4}$$

Three levels of MHD

1. ***Hydrodynamics: Eq.(1.1) (without Lorentz force) and Eq.(1.2). Inertia is important.***
2. ***MHD of liquid metals and of 3-D numerical plasma codes***
3. ***Tokamak MHD - highly anisotropic plasma with negligible inertia.***

The distance between first two is smaller than between the second and the third.

2 Large disruption on JET (1995)

Community adopted halo current explanation have been ruled out unambiguously

Vessel current during VDE, #38070

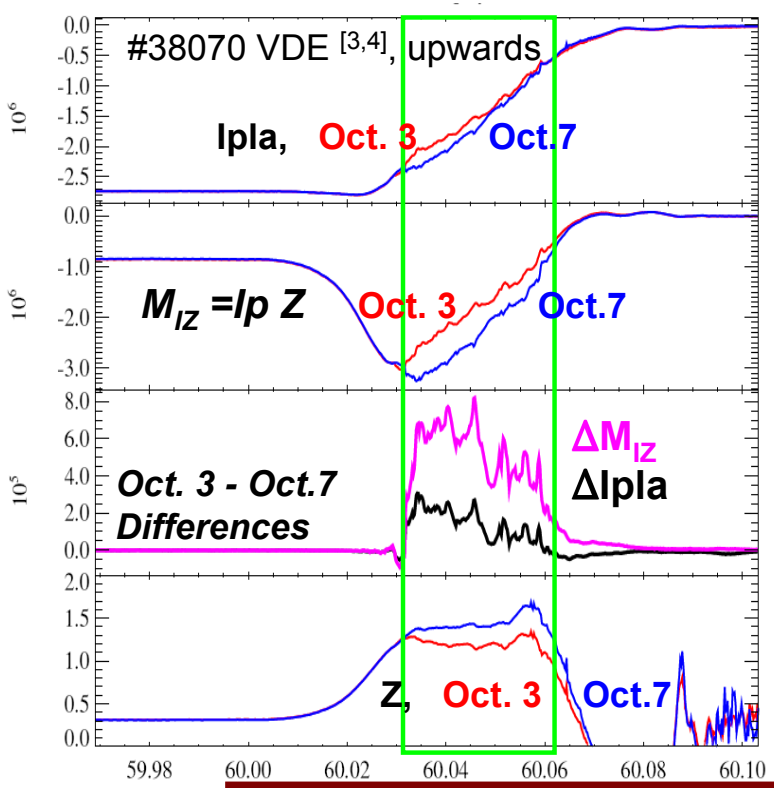

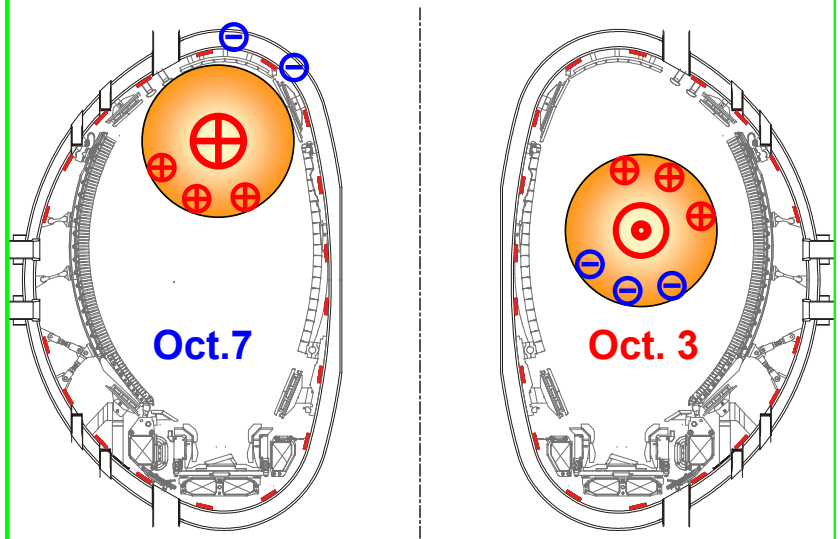

- In octant 7 the plasma is closer to top of the vessel than in octant 3.
- **The current from plasma flows on vessel in octant 7.**

The measured Ipla in octant 7 is higher then in octant 3 ➔ the missing vessel current in octant 7 is OPPOSITE to Ipla!

The "halo" current based interpretation predicts the opposite sign of asymmetry in the current measurement and contradicts JET Ipla's.

UKAEA

S N Gerasimov et al, Scaling JET Disruption Data to ITER. W70 7/10/09 8/24

Force balance versus plasma inertia in disruptions

Duration of m/n=1/1 perturbation $\simeq 25$ ms

Plasma parameters:

n_e	$3 \cdot 10^{19}$	*plasma density*
ξ	0.3 *m*	*amplitude of the perturbations*
V	90 *m*^{3}	*volume of the vacuum chamber*

Force of plasma inertia

$$F_a \simeq m_i n_i \cdot V \cdot \frac{2\xi}{(\Delta t)^2} \simeq 2 \cdot 1.7 \cdot 10^{-27} \cdot 3 \cdot 10^{19} \cdot 90 \cdot \frac{0.6}{625 \cdot 10^{-6}} \simeq 0.009\ [N]. \tag{2.1}$$

The measured value of the sideways force in this shot is

2.4 MN = 2.4·10^6 N $\gg$ 0.009 [N]

- ***All existing 3-D codes are essentially hydrodynamic codes, driven by plasma inertia.***
- ***Ignoring reality 3-D numerical codes pretend to simulate the tokamak plasma.***
- ***Some of them (M3D) claim that they simulate disruptions and the sideways force in ITER. The trick M3D uses is a hidden enhancement of ITER 15 MA current to the level of 24 MA !!! and thus exposing the benign internal kink mode or m/2 = 2/1 as the reason of forces.***

Force balance was described by theory of WTKM in 2007

Hiro current theory has amazing consistency with experiment in the sign of the effect and its time dependence. No tricks are necessary.

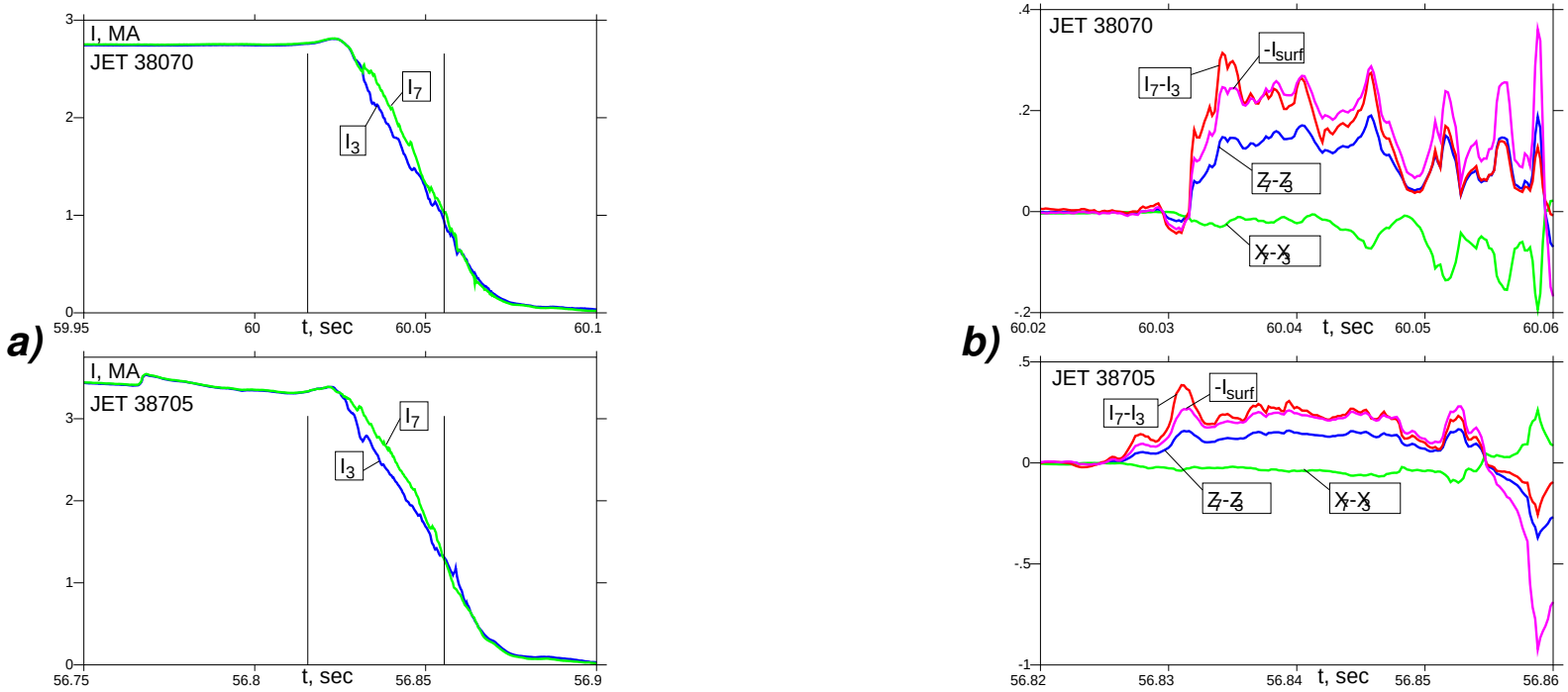

(a) Plasma currents $I_{3,7}$ in octants 3,7 on JET during the disruptions.
(b) $Z_7 - Z_3$ and $R_7 - R_3$, $I_7 - I_3$ and its prediction $-I^{surf}$ from the present theory.

$$I_{est}^{surf} \simeq -a\frac{4B_\varphi}{R_0\mu_0}\frac{\delta Z_{7,3}}{2} \ll I^{surf}, \quad Z_{7,3} \equiv \frac{1}{\mu_0 I_{pl}}\oint f B\tau dl \simeq \frac{1}{2}z_{p,7,3},$$
$$\mu_0\vec{\imath}_{11} = -2\xi_{11}\frac{B_\varphi}{R}\left(\mathrm{e}_\varphi + \frac{a}{R}\mathrm{e}_\theta\right), \quad I_{Hiro} \simeq I_{surf} = -4a\xi_{11}\frac{B_\varphi}{R\mu_0}. \qquad (2.2)$$

TMHD model: plasma & vacuum [& tiles] & wall

Duration of m/n=1/1 perturbation $\simeq 25$ ms. Where the wall currents are coming from ?

Plasma parameters:

n_e $3 \cdot 10^{19}$ - ***core plasma density***
V 90 m^3 - ***volume of the vacuum chamber***

Total electric charge in plasma particles

$$Q \simeq 2 \cdot n_e \cdot V \cdot 1.6 \cdot 10^{-19} = 3.2 \cdot 3 \cdot 10^{19} \cdot 90 \cdot 10^{-19} = 864\ [A \cdot s]. \qquad (2.3)$$

The electric charge of the shadow plasma is at least two orders of magnitude smaller than this number.

The measured charge carried by the currents from the plasma to the wall on JET

$$\int (I_7 - I_3) dt \text{ = 4350 A-s !!!}$$

There is no way to explain the tile currents in tokamaks by "halo" currents from the shadow plasma. They are not necessary for MHD dynamics and are negligible.

All currents to the tiles are coming from the plasma edge or the Scrape Off Layer established when the plasma touches the tiles. These currents (Hiro and Evans) are attributes of MHD - the instability acts as a current generator.

3 Macroscopic Tokamak MHD (TMHD)

The TMHD model utilizes the following properties of disruptions

$$\tau_{MHD} \simeq \frac{R}{V_A} = \underbrace{\frac{R}{2.18 \cdot 10^6 B/\sqrt{n}}}_{<1\ \mu s} \ll \underbrace{\tau_{TMHD}}_{\simeq 1\ ms} \ll \underbrace{\tau_{transport}}_{\simeq 0.1\ s} \ll \underbrace{\tau_{resistive}}_{\simeq 1\ s} \quad (3.1)$$

1. ***During disruptions plasma conserves magnetic fluxes. As a result, singular currents are generated at the plasma boundary and at the resonant surfaces (for*** $n \neq 0$***)***
2. ***The macroscopic tokamak plasma dynamics is driven by a small imbalance of large forces, which are much bigger than the plasma inertia. Plasma inertia is negligible (except along the resonant layers).***

- ***TMHD considers the disruption dynamics as a fast equilibrium evolution with conservation of magnetic fluxes and with singular currents.***
- ***At the same time TMHD provides the scale separation, suitable for interfacing with the non-MHD physics of singular layers and plasma edge.***

Plasma anisotropy and adaptive grids

High plasma anisotropy is the critical property of tokamaks plasma, which distinguish it from liquid metals or salt water.

TMHD expresses the anisotropy in a very simple manner, consistent with the high temperature plasma

$$(\vec{B}\cdot\nabla T_e)\simeq 0 \quad \rightarrow (\vec{B}\cdot\nabla\sigma)=0, \tag{3.2}$$

$\sigma=\sigma(T_e)$ *is the electric conductivity.*

High plasma anisotropy makes the REAL plasma behaving as ideally conducting. I fact, tokamaks are microscopically stable exclusively because of high plasma anisotropy

The hydro-dynamic numerical codes cannot implement Eq. (3.2): the problem of large 'S'. They hide the problem into the mess of "Extended MHD", which adds a train of irrelevant to dynamics terms, starting from heat conduction.

In contrast, TMHD requires adaptive grids, aligned with magnetic field:

1. *The separation of physics scales is automatic.*
2. *The interface with the non-MHD physics of resonant layers is easy.*
3. *In particular, any 'S' parameter of existing or future devices can be simulated: the higher is 'S' the better is the accuracy of TMHD*

4 Curvilinear toroidal coordinates and metric tensor

Coordinates a, θ, ζ are nested.
Nested magnetic surfaces are not required. May be ergodic.

If cylindrical coordinates are specified, e.g., by spline representation,

$$r = r(a,\theta,\zeta), \quad \varphi = \varphi(a,\theta,\zeta), \quad z = z(a,\theta,\zeta), \tag{4.1}$$

the element of the length

$$dl^2 = g_{aa}da^2 + 2g_{a\theta}dad\theta + 2g_{a\zeta}dad\zeta + g_{\theta\theta}d\theta^2 + 2g_{\theta\theta}d\theta d\zeta + g_{\zeta\zeta}d\zeta^2 \tag{4.2}$$

allows the calculations of the metric tensor

$$\begin{aligned} &g_{aa} = r_a'^2 + z_a'^2 + r^2\varphi_a', \quad g_{a\theta} = r_a'r_\theta' + z_a'z_\theta' + r^2\varphi_a\varphi_\zeta', \quad g_{a\zeta} = r_a'r_\zeta' + z_a'z_\zeta' + r^2\varphi_a\varphi_\zeta', \\ &g_{\theta\theta} = r_\theta'^2 + z_\theta'^2 + r^2\varphi_\theta', \quad g_{\theta\zeta} = r_\theta'r_\zeta' + z_\theta'z_\zeta' + r^2\varphi_\theta\varphi_\zeta', \quad g_{\zeta\zeta} = r_\zeta'^2 + z_\zeta'^2 + r^2\varphi_\zeta'. \end{aligned} \tag{4.3}$$

The Jacobian $J = \sqrt{g}$ of the metric tensor can be calculated in a straightforward manner

$$J = \sqrt{g} \equiv \frac{D(r,\varphi,z)}{D(a,\theta,\zeta)}. \tag{4.4}$$

For the case when $\zeta = \varphi$ the Jacobian has a form, similar to the two dimensional case

$$\sqrt{g} = rD, \quad D \equiv -\frac{D(r,z)}{D(a,\theta)}. \tag{4.5}$$

Important combinations of the metric tensor

$$M \equiv \frac{g_{aa}}{J}, \quad N \equiv \frac{g_{a\theta}}{J}, \quad K \equiv \frac{g_{\theta\theta}}{J}, \quad \tilde{M} \equiv \frac{g_{a\zeta}}{J}, \quad \tilde{N} \equiv \frac{g_{\theta\zeta}}{J}, \quad Q \equiv \frac{g_{\zeta\zeta}}{J}. \tag{4.6}$$

Simplest representation of confinement magnetic fields

From the property of $\nabla \cdot \vec{B} = 0$, the magnetic field can be expressed in terms of a vector potential $\vec{A}$

$$\vec{B} = (\nabla \times \vec{A}). \tag{4.7}$$

Its covariant representation in a curvilinear coordinates a, θ, ζ

$$\vec{A} = A_a \nabla a + A_\theta \nabla \theta + A_\zeta \nabla \zeta + \nabla u. \tag{4.8}$$

Utilization of freedom in the choice of $u(a, \theta, \zeta)$ gives the most compact form of the vector potential $\vec{A}$ in a given coordinate system

$$\vec{A} = -\bar{\Phi}' \eta \nabla a + (\bar{\Phi} + \phi) \nabla \theta + (\bar{\Psi} + \psi) \nabla \zeta,$$
$$\bar{\Phi} = \bar{\Phi}(a), \quad \phi = \phi(a, \zeta), \quad \bar{\Psi} = \bar{\Psi}(a), \quad \eta = \eta(a, \theta, \zeta), \quad \psi = \psi(a, \theta, \zeta). \tag{4.9}$$

The transformation of angles

$$\theta = \bar{\theta} + \frac{\bar{\Phi}'}{\bar{\Phi}' + \phi'_a} \eta, \quad \zeta = \bar{\zeta}, \tag{4.10}$$

leads to the following representation of the vector potential

$$\vec{A} = \nabla \left(\frac{\bar{\Phi}' \phi + \bar{\Phi} \phi'_a}{\bar{\Phi}' + \phi'_a} \eta \right) + (\bar{\Phi} + \phi) \nabla \bar{\theta} + \left(\bar{\Psi} + \psi - \frac{\bar{\Phi}' \phi'_{\bar{\zeta}}}{\bar{\Phi}' + \phi'_a} \eta \right) \nabla \bar{\zeta}. \tag{4.11}$$

The first term can be dropped

$$\vec{A} = (\bar{\Phi} + \phi) \nabla \bar{\theta} + \left(\bar{\Psi} + \psi - \frac{\bar{\Phi}' \phi'_{\bar{\zeta}}}{\bar{\Phi}' + \phi'_a} \eta \right) \nabla \bar{\zeta}, \tag{4.12}$$

thus, making $a, \bar{\theta}, \bar{\zeta}$ "straight field lines" coordinates in an imperfect confinement field.

5 3-D Reference Magnetic Coordinates (RMC)

RMC simplify $\vec{A}$ by massaging toroidal coordinate surfaces

$$a^{n+1} = a^n + \xi. \tag{5.1}$$

The goal is to eliminate the normal component of the magnetic field B^a

$$(\vec{B}\cdot\nabla(a+\xi)) = 0, \quad (\vec{B}\cdot\nabla\xi)^{n+1} = -B^{a,n}. \tag{5.2}$$

The ϕ, ψ terms in $\vec{B}$ in the left hand side are neglected as the higher order corrections.

The equation for ξ is reduced to a magnetic differential equation (MDE) for ξ

$$J(\vec{B}\cdot\nabla\xi) = \bar{\Phi}'(1+\eta'_\theta)\xi'_\zeta - (\bar{\Psi}' + \bar{\Phi}'\eta'_\zeta)\xi'_\theta = \phi'_\zeta - \psi'_\theta. \tag{5.3}$$

MDE can be solved in Fourier space

$$\begin{aligned} &\bar{\theta} \equiv \theta + \eta, \\ &\xi = \sum \xi_{mn}(a) e^{im\bar{\theta} - in\zeta}, \quad \psi = \sum \psi_{mn}(a) e^{im\bar{\theta} - in\zeta}, \quad \phi = \sum \phi_n(a) e^{-in\zeta}. \end{aligned} \tag{5.4}$$

This gives

$$(m\bar{\Psi}' + n\bar{\Phi}')\xi_{mn} = m\psi_{mn} - \delta^0_m n\phi_n, \quad \xi_{m'n'} = \frac{m'\psi_{m'n'} - \delta^0_{m'} n'\phi_{n'}}{m'\bar{\Psi}' + n'\bar{\Phi}'}, \tag{5.5}$$

where m', n' are non-resonant harmonics. The resonant harmonics are ignored

$$\xi_{m^*n^*} = 0 \tag{5.6}$$

A Newton scheme for building RMC

The RMC are generated by advancing the coordinate system using exclusively non-resonant components of ξ and ignoring the resonant terms.

RMC are denoted as $\bar{a}, \theta, \zeta$.

As a result of successive application of this Newton algorithm, the coordinate system is deformed $a \to \bar{a}$ in a such way, that the vector potential acquires the simplest representation, achievable without massaging the angles of coordinates.

$$\vec{A} = -\bar{\Phi}'\eta\nabla\bar{a} + \bar{\Phi}(\bar{a})\nabla\theta + \hat{\Psi}^*\nabla\zeta,$$

$$\hat{\Psi}^* \equiv \bar{\Psi}(a) + \psi^*, \quad \psi^* = \sum_{m^*n^*} \psi_{m^*n^*}(\bar{a}) e^{im^*\bar{\theta} - in^*\zeta}, \tag{5.7}$$

where ψ^* contains only resonant terms.

In straight field line coordinates $\bar{a}, \bar{\theta}, \bar{\zeta}$

$$\vec{A} = \bar{\Phi}(\bar{a})\nabla\bar{\theta} + \hat{\Psi}^*\nabla\bar{\zeta},$$

$$\hat{\Psi}^* \equiv \bar{\Psi}(\bar{a}) + \psi^*, \quad \psi^* = \sum_{m^*n^*} \psi_{m^*n^*}(\bar{a}) e^{im^*\bar{\theta} - in^*\bar{\zeta}}, \tag{5.8}$$

Magnetic islands in RMC

The resonant terms in ψ^* produce magnetic islands.

The following local flux function $\hat{\Psi}^*_{mn}$ determines the nested surfaces around the resonant magnetic field lines:

$$\hat{\Psi}^*_{nm} \equiv \bar{\Psi}^*_{mn} + \left(\psi^*_{mn} e^{im\bar{\theta}-in\zeta} + c.c.\right) = \textit{const}, \quad \bar{\Psi}^*_{mn} \equiv \bar{\Psi} + \frac{n}{m}\bar{\Phi}. \tag{5.9}$$

It is straightforward to show that

$$(\vec{B}\cdot\nabla\hat{\Psi}^*_{mn}) = 0 \tag{5.10}$$

and, thus, there is no normal component of the magnetic field to the surfaces $\bar{\Psi}^*_{n,m}$ =const.

The expansion of $\hat{\Psi}^*_{mn}$ near the resonant point $\bar{a}_{mn}$, where $\bar{\Psi}'^*_{mn} = 0$,

$$x \equiv \bar{a} - \bar{a}_{mn}, \quad \hat{\Psi}^*_{nm} = \bar{\Psi}^*_{mn} + \frac{1}{2}\bar{\Psi}''^*_{mn}x^2 + 2|\psi^*_{mn}|\cos m\beta, \quad \beta \equiv \theta - \frac{n}{m}\zeta + \alpha, \tag{5.11}$$

determines the island geometry

$$x^2 = \frac{2(\hat{\Psi}^*_{nm} - \bar{\Psi}^*_{mn})}{\bar{\Psi}''^*_{mn}} - \left|\frac{4\psi^*_{mn}}{\bar{\Psi}''^*_{mn}}\right| + \left|\frac{8\psi^*_{mn}}{\bar{\Psi}''^*_{mn}}\right| \begin{cases} \sin^2\dfrac{m\beta}{2}, & \textit{for} \quad \bar{\Psi}''^*_{mn} > 0 \\ \cos^2\dfrac{m\beta}{2}, & \textit{for} \quad \bar{\Psi}''^*_{mn} < 0 \end{cases}. \tag{5.12}$$

This gives the following value for the island width W_{mn}

$$W_{mn} = 2w_{mn} = 4\sqrt{\left|\frac{2\psi^*_{mn}}{\bar{\Psi}''^*_{mn}}\right|}, \quad \bar{\Psi}^*_{mn} = \bar{\Psi} + \frac{n}{m}\bar{\Phi}. \tag{5.13}$$

6 The set of TMHD equations

TMHD is presented by the following set of equations

1. *Equation of motion is split into an equilibrium equation*

$$\nabla p = (\vec{\jmath} \times \vec{B}), \quad \bar{\Psi} = \bar{\Psi}(\bar{\Phi}), \tag{6.1}$$

and plasma boundary advancing equation

$$\lambda \vec{\xi} = -\frac{\bar{F}}{r^2}\nabla \tilde{F}, \quad \left(\nabla \cdot \frac{\bar{F}^2}{r^4}\nabla \tilde{F}\right) = 0. \tag{6.2}$$

2. *Faraday's (Ohm's) law (the resistive part of TMHD)*

$$-\frac{\partial \vec{A}}{\partial t} - \nabla \varphi^E + (\vec{V} \times \vec{B}) = \frac{\vec{\jmath}^{pl}}{\sigma^{pl}}, \quad \vec{V} \equiv \frac{d\vec{\xi}}{dt}. \tag{6.3}$$

3. *Plasma anisotropy*

$$\sigma = \sigma(\bar{\Phi}), \quad (\vec{B} \cdot \nabla) \simeq 0. \tag{6.4}$$

4. *boundary condition at the wall*

$$\vec{E}^{pl}_{\|} = \vec{E}^{wall}_{\|} = \frac{\vec{\jmath}^{pl}}{\sigma^{pl}} - (\vec{V} \times \vec{B}) = \frac{\vec{\jmath}^{wall}}{\sigma^{wall}}. \tag{6.5}$$

Force balance across the free plasma surface

$$\left(p + \frac{|\vec{B}|^2}{2\mu_0} + \frac{\bar{F}\tilde{F}}{r^2\mu_0}\right)_i = \left(\frac{|\vec{B}|^2}{2\mu_0}\right)_e, \tag{6.6}$$

where subscripts 'i, e' specify the inner and outer sides of the plasma surface.

6.1 The physics behind TMHD

- *Flux conserving equilibrium evolution automatically generates the surface currents (mostly in toroidal direction) at the plasma-vacuum interface*
- *The plasma core is kept in equilibrium, but there is a force acting on the surface currents.*
- *In response the plasma generates poloidal currents $\delta\vec{j}_{pol}$ which enters the plasma boundary normally and create and additional surface currents.*
- *As a result, the total surface current (including poloidal current distribution) becomes force-free.*
- *The $(\delta\vec{j}\times\vec{B})$ force in the core is balanced by a plasma inertia (or by friction force in TMHD model).*
- *Two first equations of TMHD determine a unique sequence of equilibrium configurations, independent on the plasma resistivity or plasma-wall interactions*

  This is a very important property for comparison with experiments and revealing the non-ideal plasma properties.
- *It is Faraday's law which determines the time moment for each configurations.*

The proper splitting of MHD equation of motion eliminates very restrictive Courant condition for the time step in MHD simulations.
It also allows the use of plasma inertia in the plasma advancing equation without limitations of the time step.

6.2 Plasma advancing equation

In TMHD, the "equation of motion" (6.2) is treated in an approximate way, assuming small plasma deformation δa with respect to the major radius r

$$\left(\frac{\delta a}{r}\right)^2 \ll 1, \quad \left(\frac{\partial}{\partial \zeta}\right) \ll \left(\frac{\partial}{\partial \theta}\right), \quad \left(\frac{\partial}{\partial \zeta}\right) \ll a\left(\frac{\partial}{\partial a}\right). \tag{6.7}$$

This approximation may slightly affect the shape of the plasma but keeps all physics effects related to disruptions.

The perturbed current density in TMHD is given by

$$\delta\vec{j} = (\nabla\tilde{F} \times \nabla\zeta). \tag{6.8}$$

The associated Lorentz force

$$(\delta\vec{j} \times \vec{B}) \simeq \left((\nabla\tilde{F} \times \nabla\zeta) \times (JB^{\zeta}(\nabla a \times \nabla\theta))\right) \simeq -B^{\zeta}\nabla\tilde{F} \simeq -\frac{\bar{F}}{r^2}\nabla\tilde{F}. \tag{6.9}$$

The perturbation of $\tilde{F}$ is determined by the condition that the virtual plasma displacement $\vec{\xi}$ does not perturb the toroidal magnetic field at the level larger than it was considered for the Lorentz force.

$$\tilde{B}_{tor} = (\nabla \times (\vec{\xi} \times \vec{B}))_{tor} = 0, \quad \left(\nabla \cdot \frac{\bar{F}}{r^2}\vec{\xi}\right) = -\left(\nabla \cdot \frac{\bar{F}^2}{r^4}\nabla\tilde{F}\right) = 0 \tag{6.10}$$

The approximations here are used exclusively for describing the inertial term, which in reality is small and does not need excessive precision. It simply determines a relaxation process (one of them) for finding the final equilibrium which evolves at intermediate resistive-inertial time scale.

6.3 3-D equilibrium in the Grad-Shafranov form

The contravariant components of $\vec{B}$

$$B^a = \frac{\psi'_\theta - \phi'_\zeta}{J}, \quad B^\theta = -\frac{\bar{\Psi}' + \psi'_a + \bar{\Phi}'\eta'_\zeta}{J}, \quad B^\zeta = \frac{\bar{\Phi}'(1+\eta'_\theta) + \phi'_a}{J} \tag{6.11}$$

and the covariant components of the magnetic field

$$\vec{B} \equiv -\nu\nabla a + \hat{J}\nabla\theta + \hat{F}\nabla\zeta + \nabla\sigma, \quad \hat{J} = \hat{J}(\bar{a},\zeta). \tag{6.12}$$

Covariant components can be expressed in terms of components of the vector potential

$$\begin{aligned}
B_a &= M(\psi'_\theta - \phi'_\zeta) - N(\bar{\Psi}' + \psi'_a + \bar{\Phi}'\eta'_\zeta) + \tilde{M}[\bar{\Phi}'(1+\eta'_\theta) + \phi'_a], \\
B_\theta &= N(\psi'_\theta - \phi'_\zeta) - K(\bar{\Psi}' + \psi'_a + \bar{\Phi}'\eta'_\zeta) + \tilde{N}[\bar{\Phi}'(1+\eta'_\theta) + \phi'_a], \\
B_\zeta &= \tilde{M}(\psi'_\theta - \phi'_\zeta) - \tilde{N}(\bar{\Psi}' + \psi'_a + \bar{\Phi}'\eta'_\zeta) + Q[\bar{\Phi}'(1+\eta'_\theta) + \phi'_a].
\end{aligned} \tag{6.13}$$

Ampere's law determines components of $\vec{A}$, given the current density

$$\begin{aligned}
&\frac{\partial}{\partial a}\left[\tilde{M}(\psi'_\theta - \phi'_\zeta) - \tilde{N}(\bar{\Psi}' + \psi'_a + \bar{\Phi}'\eta'_\zeta) + Q(\bar{\Phi}'(1+\eta'_\theta) + \phi'_a)\right] \\
&-\frac{\partial}{\partial\zeta}\left[M(\psi'_\theta - \phi'_\zeta) - N(\bar{\Psi}' + \psi'_a + \bar{\Phi}'\eta'_\zeta) + \tilde{M}(\bar{\Phi}'(1+\eta'_\theta) + \phi'_a)\right] = \hat{F}'_a + \nu'_\zeta, \\
&\frac{\partial}{\partial a}\left[N(\psi'_\theta - \phi'_\zeta) - K(\bar{\Psi}' + \psi'_a + \bar{\Phi}'\eta'_\zeta) + \tilde{N}(\bar{\Phi}'(1+\eta'_\theta) + \phi'_a)\right] \\
&-\frac{\partial}{\partial\theta}\left[M(\psi'_\theta - \phi'_\zeta) - N(\bar{\Psi}' + \psi'_a + \bar{\Phi}'\eta'_\zeta) + \tilde{M}(\bar{\Phi}'(1+\eta'_\theta) + \phi'_a)\right] = \hat{J}'_a + \nu'_\theta,
\end{aligned} \tag{6.14}$$

which determine the combinations of the unknowns $\bar{\Psi}(a)+\psi(a,\theta,\zeta)$,$\bar{\Phi}(a)+\phi(a,\zeta)$ and $\eta(a,\theta,\zeta)$ given the right hand side $\hat{J}(a,\zeta), \hat{F}(a,\theta,\zeta), \nu(a,\theta,\zeta)$.

6.4 Radial force balance outside islands

The current density at each iteration is specified in RMC, which determine island widths.

Force balance between islands (here, for simplicity we use the SFL coordinates):

$$\bar{p}'\sqrt{g} = (\bar{J}' + \nu_{\bar{\theta}})\bar{\Psi}' - (\bar{F}' + \nu_{\bar{\zeta}})\bar{\Phi}'. \tag{6.15}$$

(In RMC the term ψ^* can be made small and we neglect it in the force balance equation.)

It can be split into the averaged

$$\bar{J}'\bar{\Psi}' - \bar{F}'\bar{\Phi}' = \bar{p}'\,(\sqrt{g})_0 \tag{6.16}$$

and the oscillatory MDE equation for ν

$$\bar{\Psi}'\nu_{\bar{\theta}} - \bar{\Phi}'\nu_{\bar{\zeta}} = \bar{p}'[\sqrt{g} - (\sqrt{g})_0] = \bar{p}'\sum_{m,n}(\sqrt{g})_{mn}e^{im\bar{\theta}-in\bar{\zeta}}, \tag{6.17}$$

which can be solved in Fourier space as it was described earlier in Eqs. (5.4-5.5)

$$\bar{\nu} \equiv \sum_{m,n}\nu_{mn}e^{im\bar{\theta}-in\bar{\zeta}}, \quad \bar{\nu}_{mn} = -i\bar{p}'\frac{(\sqrt{g})_{mn}}{m\bar{\Psi}' + n\bar{\Phi}'}. \tag{6.18}$$

Given $\bar{p}'(\bar{a})$, $\bar{J}(\bar{a})$, these equations determine the RHS for Ampere's law equations outside the islands

$$(\nabla \times (\nabla \times \vec{A})) = -\mu_0\vec{j}. \tag{6.19}$$

6.5 Equilibrium current density near the islands

In the vicinity of the island m, n the shape of magnetic surfaces is described by function $\hat{\Psi}^*_{mn}(\bar{a}, \bar{\theta}, \zeta)$. The local flux coordinate χ inside the island $\hat{\Psi}^*_{mn} = \hat{\Psi}^*_{mn}(\chi)$

$$\chi^2 = \frac{2(\hat{\Psi}^*_{nm} - \bar{\Psi}^*_{mn})}{\bar{\Psi}''^*_{mn}} + \frac{w^2}{2}, \quad w^2 = \left|\frac{8\psi^*_{mn}}{\bar{\Psi}''^*_{mn}}\right|, \tag{6.20}$$

determines the geometry of the flux surfaces $x \equiv \bar{a} - \bar{a}^*$ by

$$x^2 = \chi^2 - w^2 + w^2 \begin{cases} \sin^2 \dfrac{m\beta}{2}, & \text{for} \quad \bar{\Psi}''^*_{mn} > 0, \\ \cos^2 \dfrac{m\beta}{2}, & \text{for} \quad \bar{\Psi}''^*_{mn} < 0 \end{cases}. \tag{6.21}$$

In order to describe the equilibrium current density in the vicinity of the island it is necessary to introduce a local poloidal coordinate

$$\hat{\theta} \equiv \theta - \frac{n}{m}\zeta, \quad \left(\bar{\Psi}'\frac{\partial}{\partial\theta} - \bar{\Phi}'\frac{\partial}{\partial\zeta}\right)_{\bar{a}=\bar{a}^*} \hat{\theta} = 0. \tag{6.22}$$

The equilibrium current density near the island has no normal component to the island magnetic surface $\hat{\Psi}^*_{mn}$ =const. Accordingly, it can be represented as

$$\begin{aligned} &\bar{\vec{j}} = (\nabla\hat{F}^* \times \nabla\zeta) + (\nabla\hat{J}^* \times \nabla\hat{\theta}), \\ &\hat{J}^* = \hat{J}^*(\chi, \hat{\theta}) = \bar{J}^*(\chi) + \nu^*(\chi, \hat{\theta}), \quad \bar{F}^* = \bar{F}^*(\chi, \bar{\zeta}). \end{aligned} \tag{6.23}$$

Together with the given plasma pressure $\bar{p} = \bar{p}(\chi)$ this determines the current density in vicinity of the islands.

7 Electro-magnetic model of the wall in TMHD

TMHD intends to reproduce the current sharing effect (e.g., Hiro and Evans currents) between the plasma and the wall during disruptions.

Thin wall approximation is reasonable for wall modeling. 3-D geometry of the wall is essential.

Two components in the surface current density $h\vec{j}$ ***(*** h ***is the thickness of the current distribution):***

$$h\vec{j} = \vec{\imath} - \bar{\sigma}\nabla\phi^S. \tag{7.1}$$

1. ***divergence free Hiro/eddy current:*** $\vec{\imath} \equiv \nabla I \times \vec{n}$
2. ***plasma sink/source (Evans) current*** $-\bar{\sigma}\nabla\phi^S, \quad \bar{\sigma} \equiv h\sigma$

(Here I ***is the stream function,*** ϕ^S ***is the plasma source potential,*** σ ***is electric conductivity of the wall.)***

Current sharing equation

$$(\nabla \cdot (h\vec{j})) = -(\nabla \cdot (\bar{\sigma}\nabla\phi^S)) = -j_\perp, \tag{7.2}$$

(where $j_\perp$ ***is the density of the current coming from/to the plasma.)***

Inductance equation for eddy currents

$$-\frac{\partial \vec{A}}{\partial t} - \nabla\phi^E = \bar{\eta}(\nabla I \times \vec{n}) - \nabla\phi^S, \quad \bar{\eta} \equiv \frac{1}{\bar{\sigma}} \tag{7.3}$$

is decoupled from the current sharing

$$(\nabla \cdot (\bar{\eta}\nabla I)) = \frac{\partial B_\perp}{\partial t} = \frac{\partial (B_\perp^{pl} + B_\perp^{coil} + B_\perp^I + B_\perp^S)}{\partial t}. \tag{7.4}$$

8 Energy functionals for TMHD equations

It is remarkable that each of all TMHD equations has its own energy principle leading to a positively defined symmetric matrix if expressed in terms of finite elements.

***3-D equilibrium* (3-D Hermit elements, block tri-diagonal)**

$$W^{\vec{j}\times\vec{B}} \equiv \frac{1}{2}\int\left(\frac{|\vec{B}|^2}{2\mu_0} - (\vec{A}\cdot\vec{j})\right)d^3\mathrm{r}$$
$$\equiv \frac{1}{2\mu_0}\int\Big\{K(\bar{\Psi}' + \psi'_a + \bar{\Phi}'\eta'_\zeta)^2 - 2N(\bar{\Psi}' + \psi'_a + \bar{\Phi}'\eta'_\zeta)(\psi'_\theta - \phi'_\zeta) + M(\psi'_\theta - \phi'_\zeta)^2 \quad (8.1)$$
$$+Q(\bar{\Phi}' + \phi'_a + \bar{\Phi}'\eta'_\theta)^2 - 2\tilde{N}(\bar{\Psi}' + \psi'_a + \bar{\Phi}'\eta'_\zeta)(\bar{\Phi}' + \phi'_a + \bar{\Phi}'\eta'_\theta)$$
$$+2\tilde{M}(\psi'_\theta - \phi'_\zeta)(\bar{\Phi}' + \phi'_a + \bar{\Phi}'\eta'_\theta) - (\bar{\Phi} + \phi)\hat{F}'_a + (\bar{\Psi} + \psi)(\hat{J}'_a + \nu'_\theta)\Big\}\,da d\theta d\zeta.$$

***Plasma advancing* (3-D Hermit elements, block tri-diagonal)**

$$W^F = \frac{1}{2}\int \bar{F}^2\frac{g^{aa}\tilde{F}'^2_a + 2g^{a\theta}\tilde{F}'_a\tilde{F}'_\theta + g^{\theta\theta}\tilde{F}'^2_\theta + 2g^{a\zeta}\tilde{F}'_a\tilde{F}'_\zeta + 2g^{\theta\zeta}\tilde{F}'_\theta\tilde{F}'_\zeta + g^{\zeta\zeta}\tilde{F}'^2_\zeta}{r^4}J da d\theta d\zeta. \quad (8.2)$$

***Faraday's law* (3-D Hermit elements, block tri-diagonal)**

$$W^t = \frac{1}{2}\int\left\{\frac{\partial}{\partial t}\left(KB^\theta B^\theta + 2\tilde{M}B^\theta B^\zeta + QB^\zeta B^\zeta\right) + \eta^{pl}\left(Kj^\theta j^\theta + 2\tilde{M}j^\theta j^\zeta + Qj^\zeta j^\zeta\right)\right\}d^3r. \quad (8.3)$$

***Sink/source wall current from the plasma* (triangle based wall model, sparse matrix)**

$$W^S = \int\left\{\frac{\bar{\sigma}(\nabla\phi^S)^2}{2} + j_\perp\phi^S\right\}dS - \frac{1}{2}\oint\phi^S\bar{\sigma}[(\vec{n}\times\nabla\phi^S)\cdot d\vec{l}]. \quad (8.4)$$

***Eddy currents* (triangle based wall model, stationary matrix)**

$$W^I \equiv \frac{1}{2}\int\left\{\frac{\partial(\vec{\imath}\cdot\vec{A}^I)}{\partial t} + \bar{\eta}|\nabla I|^2 + 2\left(\vec{\imath}\cdot\frac{\partial\vec{A}^{ext}}{\partial t}\right)\right\}dS - \oint(\phi^E - \phi^S)\frac{\partial I}{\partial l}dl. \quad (8.5)$$

8.1 Numerical scheme of TMHD (used in 2-D EEC&VDE)

By appropriate enumeration, for both 2- and 3-D cases, the resulting matrix can represented as a block-tri-diagonal cycle matrix

This structure can be utilized for developing an efficient direct solver

- ***First, a block-tri-diagonal algorithm was implemented as a first solver of matrix equation***
- ***Second, faster Cholesky decomposition scheme was developed to utilize advantages of matrix structure***

$$A = LL^T. \tag{8.6}$$

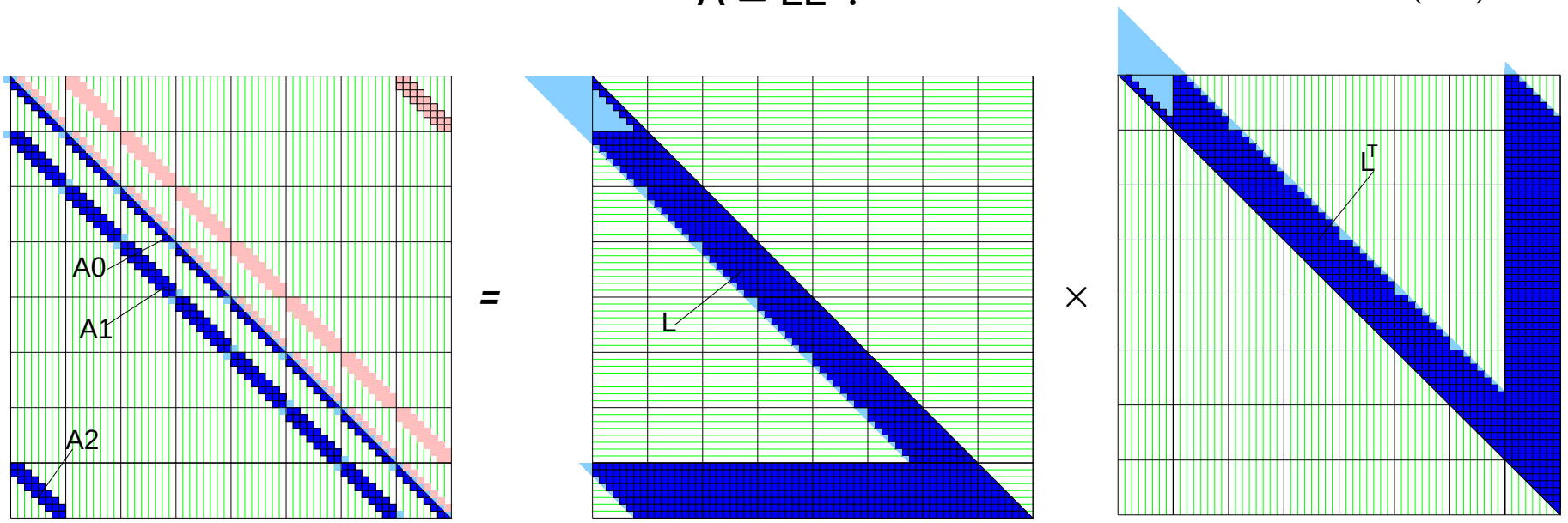

Original matrix L ***factor*** L^T ***factor***

EEC uses the same ESC algorithm, $\xi\bar{\Psi}'_0 = -\psi$, for grid advancing

8.2 Free-boundary equilibria with ESC-EEC

ESC-EEC can calculate free-boundary equilibria in both $r - z$ and flux coordinates

The Equilibrium Spline Interface (ESI) is developed for equilibrium codes instead of present mess in interfacing

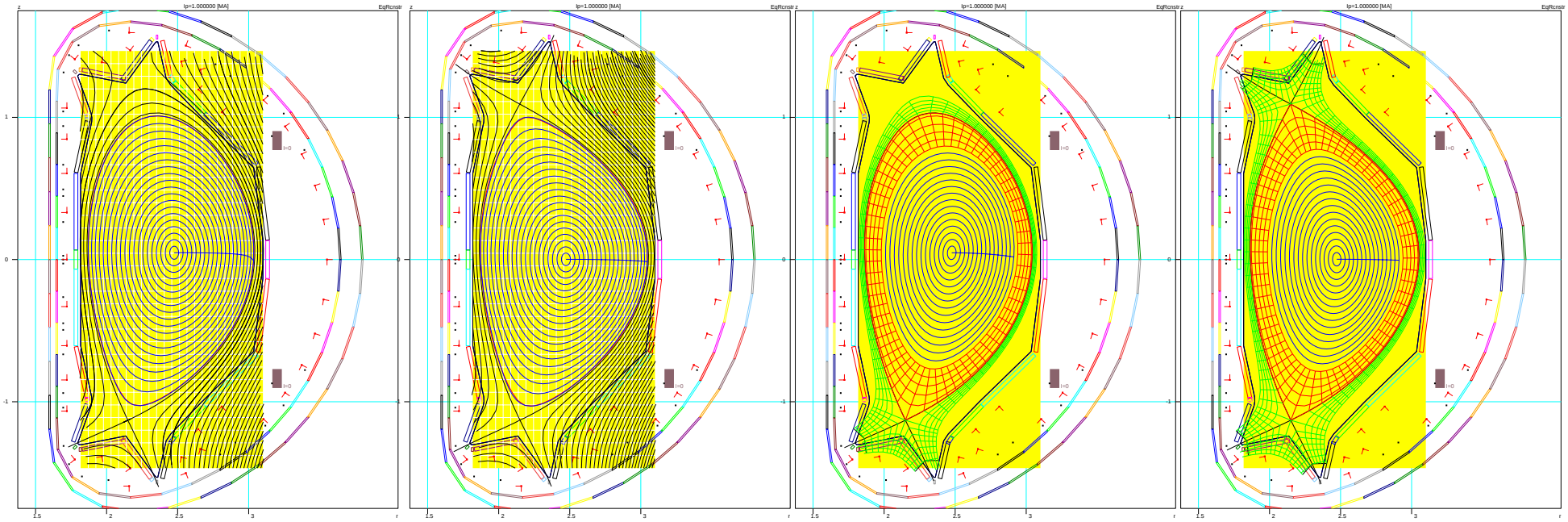

(a) ID=00,1,00,00,00 (b) ID=00,01,00,00,00 (c) ID=00,40,00,00,23 (d) ID=00,40,00,00,23

Examples of EAST free boundary equilibrium configurations with (a,c) single and (b,d) double null separatrixes calculated by ESC-EEC.

a),b) Interface IDs for equilibria with $r - z$ coordinate data;

(c),d) ESI IDs for equilibria with the core, edge and vacuum flux coordinate data

8.3 TMHD in vertical disruptions

In tokamaks, the plasma is always "separated" from the wall based on $\Psi_{pl}, \Psi_X, \Psi_{Wall}$.

The presence of the wall does not affect VDE significantly

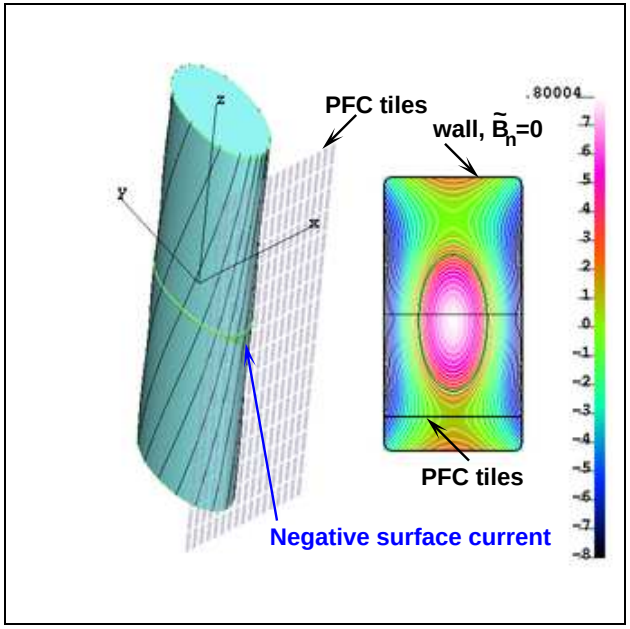

Initial plasma displacement

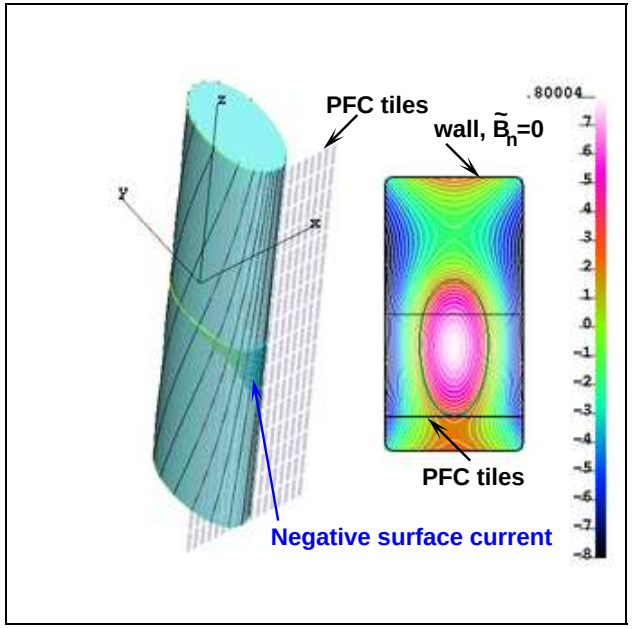

Negative surface current at the leading edge

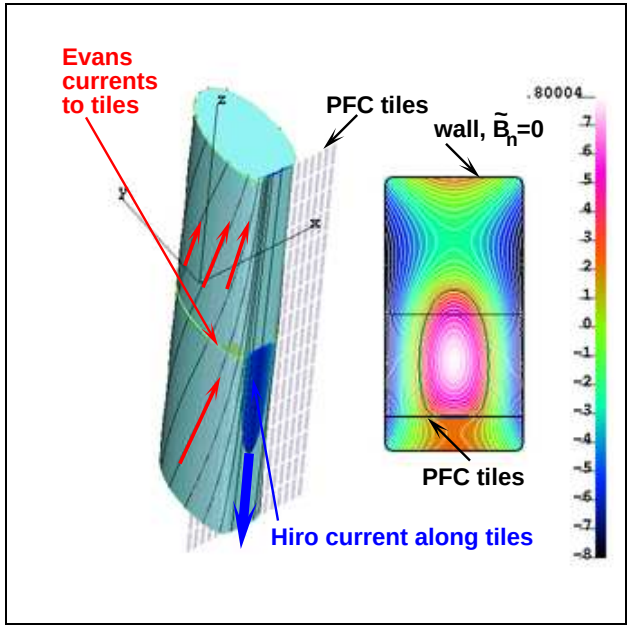

Hiro, Evans currents, formation of two Y-points

Predicted by the TMHD theory
(a) surface currents at the plasma boundary
(b) Hiro currents along the tile surface in the toroidal direction
(c) Evans currents from the plasma edge to the tile surface are well reproduced by the new VDE code.

Intermediate equilibrium maintained by the Hiro currents

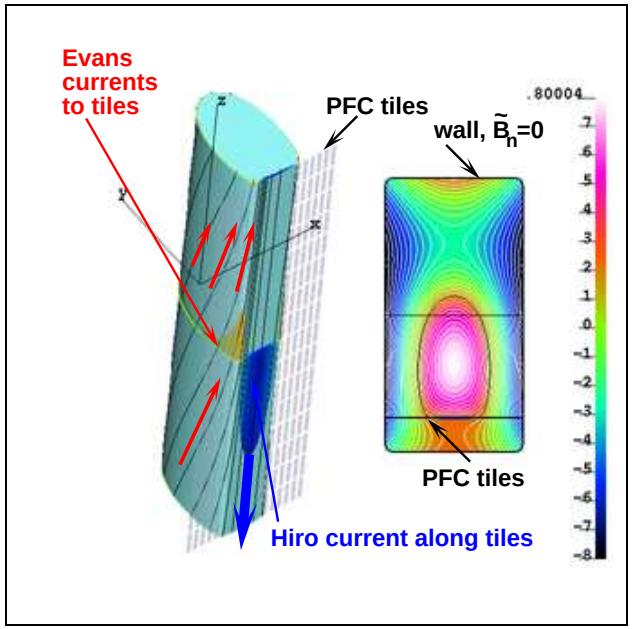

Hiro currents apply the force to tiles

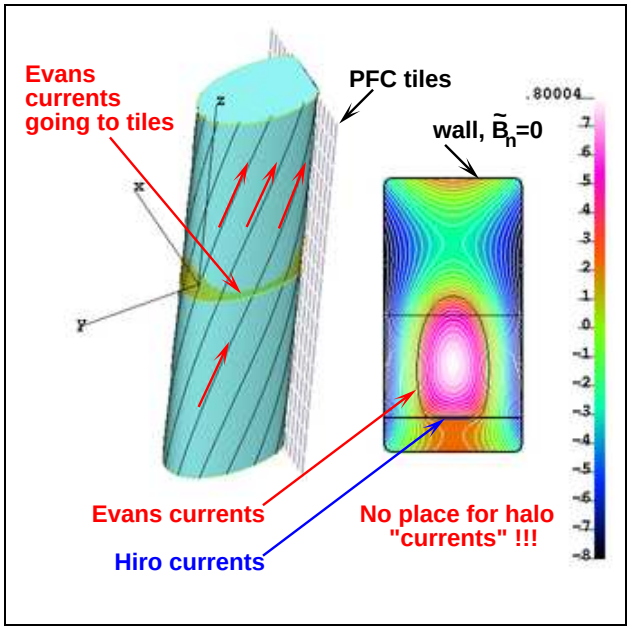

Evans currents. No place for fake "halo" currents

Plasma shrinking due to decay of Hiro currents

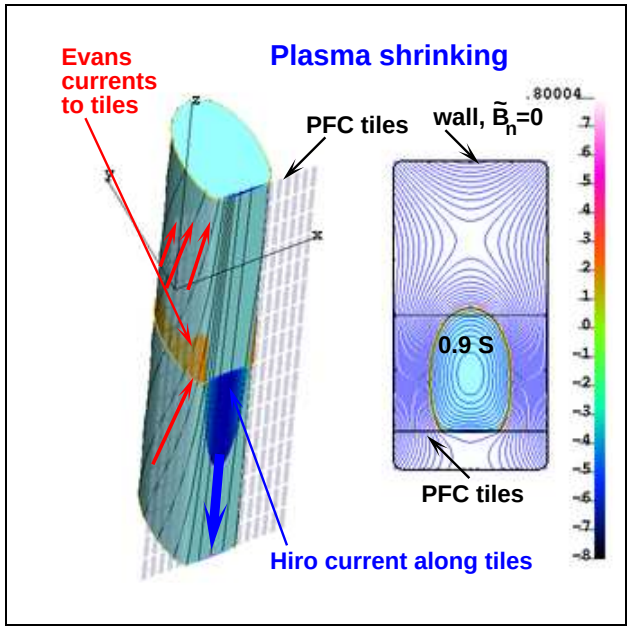

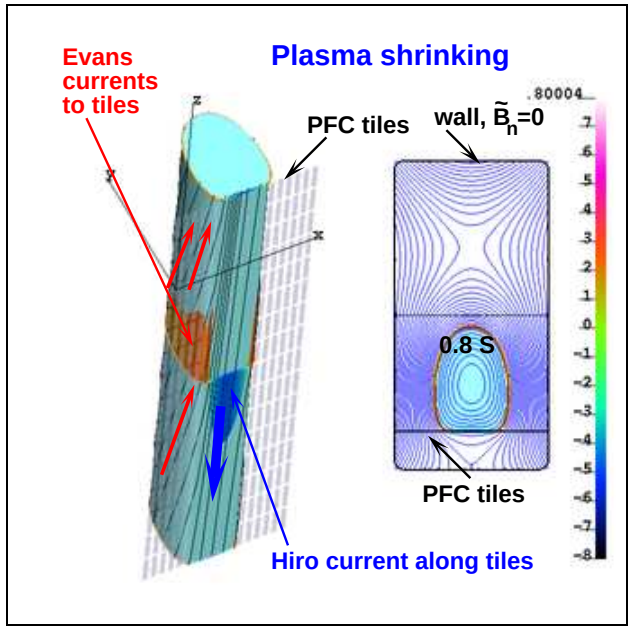

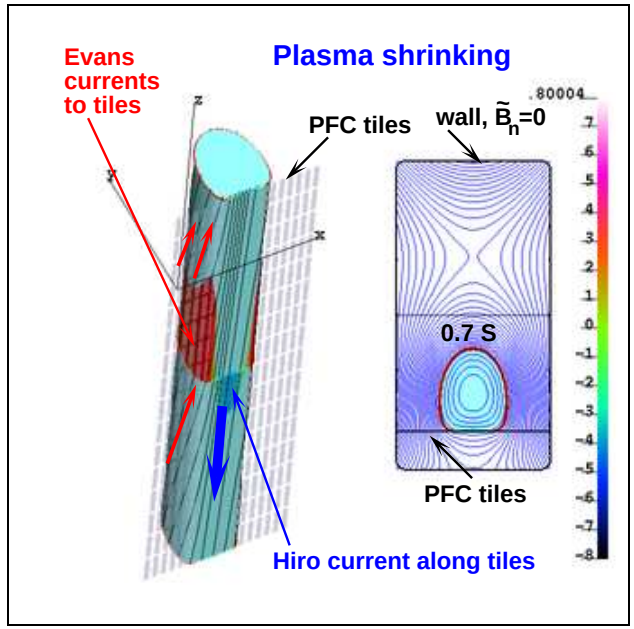

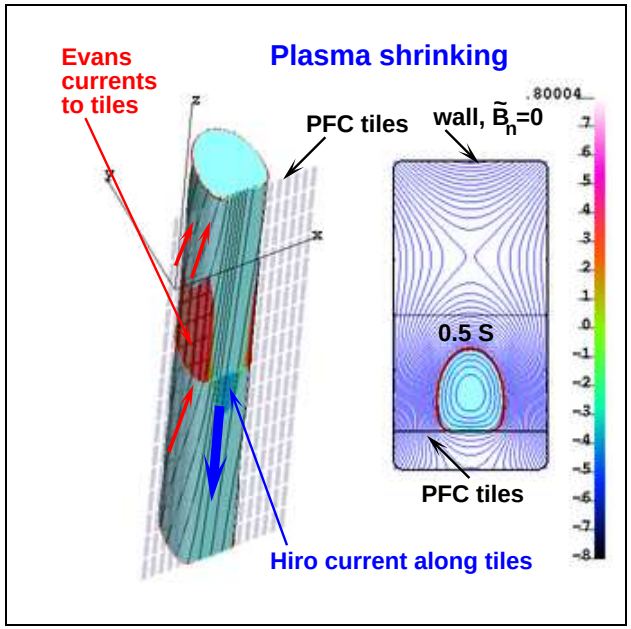

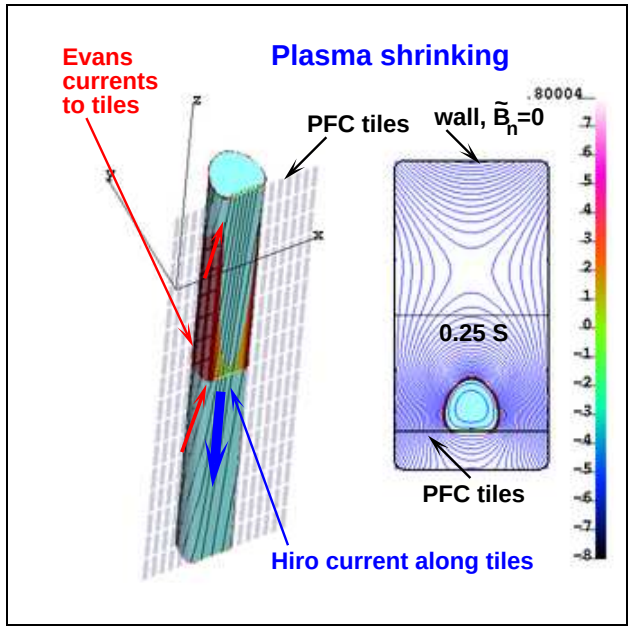

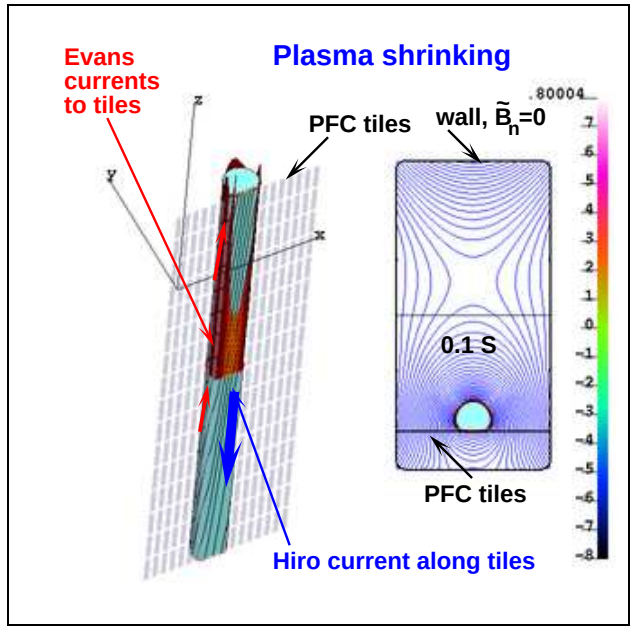

TMHD challenges the community regarding tile currents 29/33

The physics of VDE was significantly confused in 1991 (Strait et al, Nucl. Fus. 1991) where currents to the tiles were discovered.

The misuse of EFIT reconstruction code led to misinterpretation of these electric currents as "halo" currents.

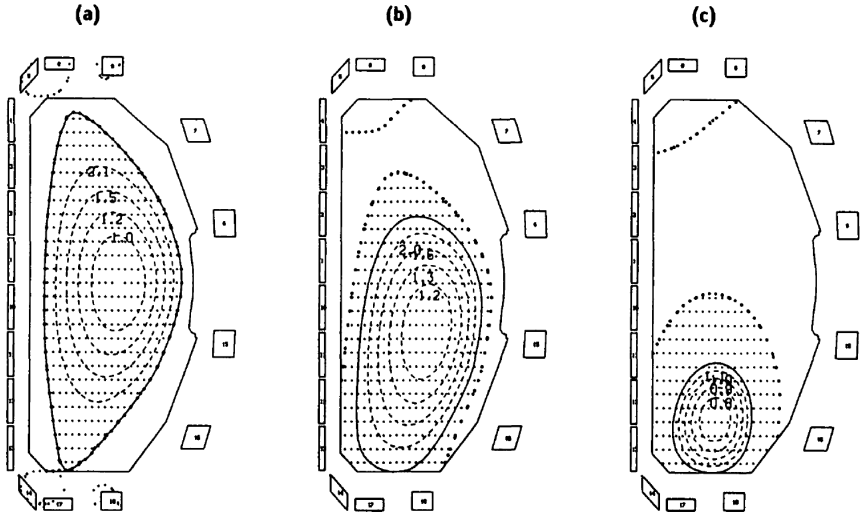

FIG. 3. Equilibrium flux plots from EFIT at three times during the vertical instability: (a) 2660 ms, (b) 2675 ms and (c) 2684 ms. Plasma current was allowed in the hatched region, including part of the SOL.

Figure 1: EFIT reconstruction of plasma configuration in VDE

Despite of wide acceptance by fusion community, the physics picture supporting the halo-current interpretation was never established.

In fact, the model is in strong contradiction with every direct measurement (JET, EAST).

Evans currents, predicted by TMHD, rather than ghost of "halo" currents, are the tile currents measured by experiment.

VDE simulations motivate innovative diagnostics

We suggested a comprehensive set of innovative tile diagnostics for Hiro, Evans and SoL current measurements on NSTX-U

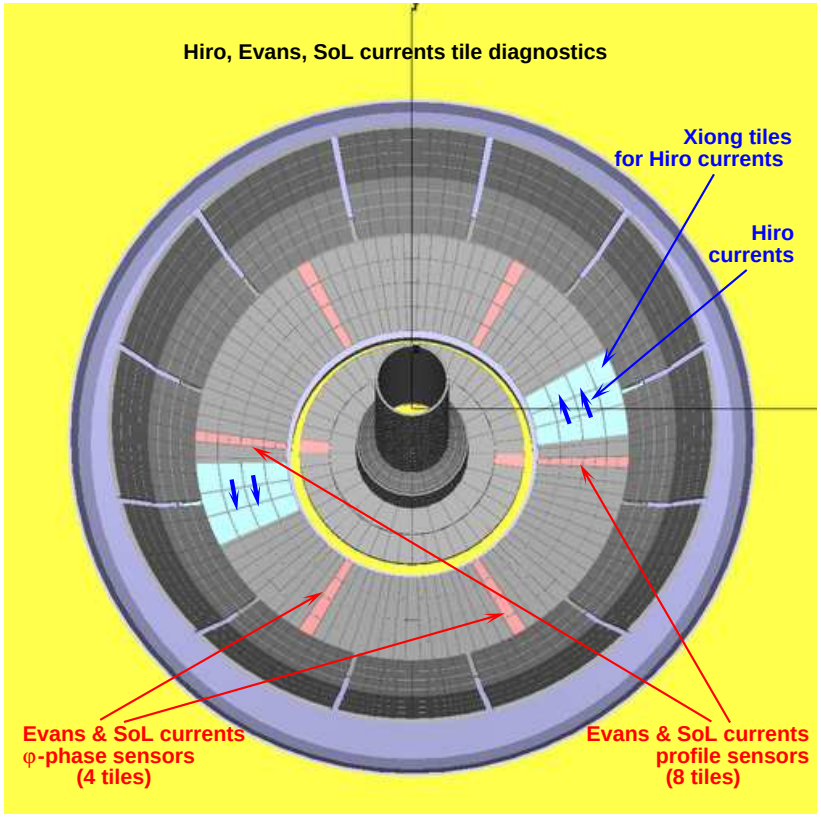

Tile sensors for measuring Hiro, Evans, and SoL currents and different kinds of diagnostics including

1. ***Hiro current diagnostics***
2. ***Evans current profile diagnostics with enhanced radial resolution***
3. ***Evans current φ-phase diagnostics***
4. ***SoL current measurements***

Evans currents carry important information on plasma-PFC interactions, never touched

VDE code for EAST

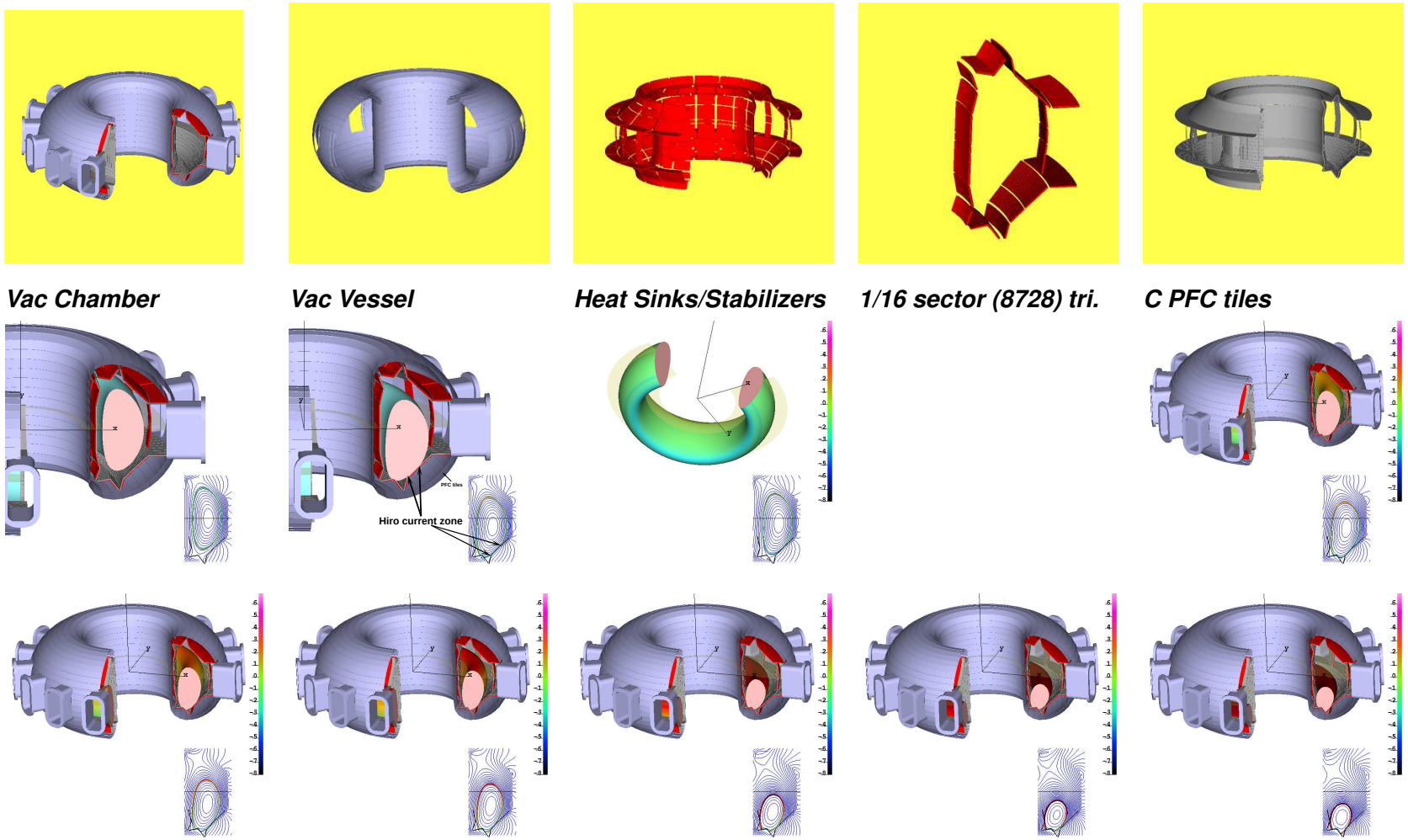

In simulations plasma generate the Hiro currents in the same locations as Hiro current measurements.

9 TMHD and progress in disruption understanding

TMHD model was initiated and validated in 2007 by a creation of theory of Hiro currents, which explained the plasma current asymmetry in JET disruptions

This progress was not matched by numerical simulations, which fell short in addressing the practical needs of the next step fusion device ITER in resolving the disruption problem.

Now it became clear that it is not possible to move forward based on hydro-dynamic approaches of the present numerical codes. The deceptive practice of M3D simulations is an extreme example of their failure.

TMHD puts numerical simulations into consistency with theoretical understanding and experimental observations.

1. ***Reference Magnetic Coordinates resolve the long standing problem of practical coordinates for stochastic and ergodic magnetic fields. They establish the numerical consistency with high anisotropy of the tokamak plasma.***
2. ***TMHD makes proper consideration of the equation of motion for plasma and resolves the long standing problem in MHD codes related to Courant limitation of the time step.***
3. ***The TMHD model contains a reasonably realistic wall model and (a) eddy and (b) additional sink/source currents***
4. ***All partial differential equations of TMHD have energy functionals, leading to efficient and stable computations, suitable for the use of GPU.***
5. ***TMHD predicts a unique sequence of equilibrium configurations, which would help to reveal the physics of the plasma edge and plasma-wall interactions.***

TMHD gives the science based explanation of tile currents, measured in tokamaks during VDE, as the Evans currents

Upon necessity (for plasma control or reconstruction purposes), TMHD equations can be solved in r, ϕ, z coordinates with use of RMC for specification of current density only.

10 Summary

TMHD model finally addresses the long term overdue problem of developing numerical MD codes for the high temperature tokamak plasma: 2D ESC-EEC, VDE, DSC are operational

Basics TMHD was understood in 2007:

- *Any plasma deformation excites the surface currents at the plasma*
- *Plasma goes to a slowdown evolution when negative surface currents are converted into as Hiro currents at the wall*
- *Wall Touching Kink and Vertical Modes are introduced into theory*

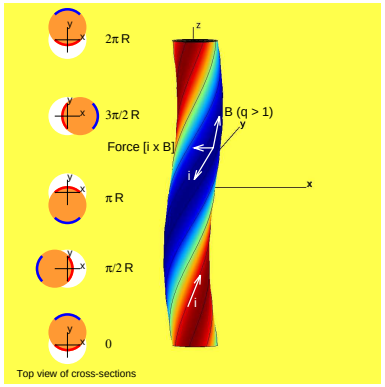

m/n=1/1 surface currents

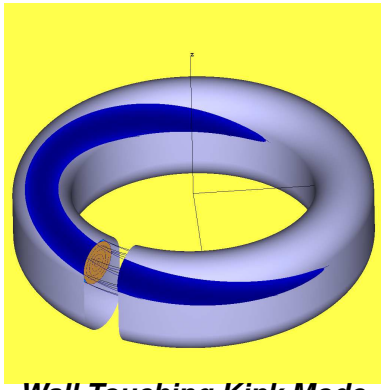

Wall Touching Kink Mode (JET)

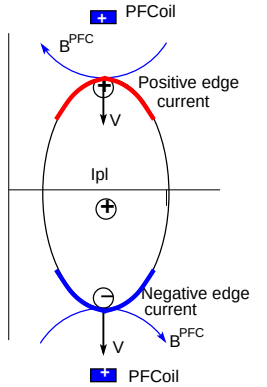

Surface currents in VDE

Successes of TMHD:

- *100 % success in explanation of the sign of toroidal asymmetry δI_{pl} in plasma current in JET VDE*
- *Prediction of Hiro currents in axisymmetric Vertical Disruption Event (VDE)*
- *Design of a special tile diagnostics and first measurements of Hiro currents in VDE on EAST.*
- *Dismissal of halo" currents and Evans currents based of VDE measurements in tokamaks*

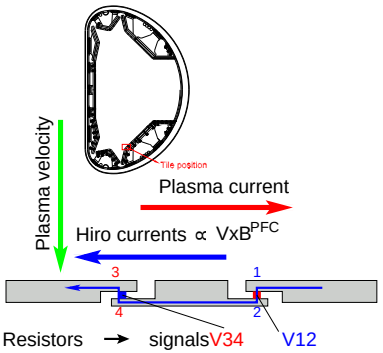

4 types of currents can be distinguished on EAST

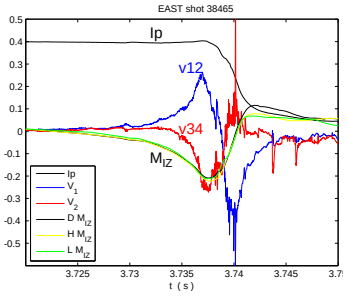

Downward VDE generates Hiro currents

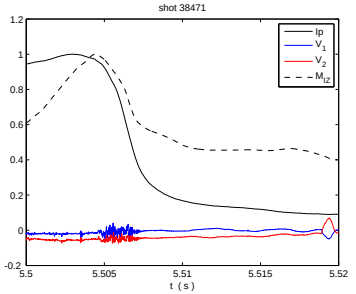

Upward VDE does not produce a signal

The EAST measurements have confirmed the critical prediction of TMHD:

Plasma motion to the plates is necessary for excitation of Hiro currents